Journal of Experimental Botany, Vol. 44, No. 265, pp. 1369–1375, August 1993

Electrical Impedance Analysis in Plant Tissues: Impedance Measurement in Leaves

M. I. N. ZHANG[1] and J. H. M. WILLISON

Department of Biology, Dalhousie University, Halifax, N.S. Canada B3H 4J1

Received 7 October 1992; Accepted 13 May 1993

ABSTRACT

Electrical impedance spectra (100 Hz–800 kHz) were measured in leaves of *Peperomia obtusifolia* L. (a succulent) and *Brassica oleracea* L. (cabbage). By measuring impedances at three or more inter-electrode distances in a single leaf, electrode impedance and specific tissue impedance were separated.

Analysis of impedance data from *B. oleracea* leaves in relation to an equivalent circuit model showed that leaf development was accompanied by increases in extracellular resistance, cytoplasmic resistance and vacuole interior resistance, together with decreases in plasma membrane capacitance and tonoplast capacitance. After *B. oleracea* leaves were subjected to a −6 °C freeze–thaw stress, extracellular resistance, cytoplasmic resistance and vacuole interior resistance decreased, but plasma membrane capacitance and tonoplast capacitance did not change. These results indicate that useful measurements of leaf parameters can be obtained by this technique.

Examination of the electrode impedance spectrum showed that electrode insertion produced a damaged collar, 0·4–0·5 mm wide, around the electrode. This was confirmed by visual observation of the damage in *P. obtusifolia* leaf.

Key words: *Peperomia obtusifolia* L., *Brassica oleracea* L. (cabbage), electrical impedance, equivalent circuit, electrode polarization.

INTRODUCTION

Measurement of electrical impedances in plant tissues has long been considered a technique with useful potential in plant physiology (for review, see Wilner and Brach, 1979; Ackmann and Seitz, 1984), but practical results have sometimes been disappointing. Nevertheless, the ability to make measurements from living tissue with minimal damage continues to make research into the methodology attractive (Stout *et al.*, 1987; Zhang and Willison, 1991*a*, *b*). In the past, most measurements have been made on bulk tissues (Hayden *et al.*, 1969; Ackmann and Seitz, 1984; Stout *et al.*, 1987; Repo *et al.*, 1990), although some attempts have also been made to make measurements in laminar organs, notably leaves (Greenham *et al.*, 1972, 1978, 1980).

Like impedance measurement in bulk tissues, impedance measurement in leaves is complicated by the presence of electrode impedance that results from electrode polarization if a two-terminal electrode arrangement is used (Schwan, 1963; Ferris, 1974; Ackmann and Seitz, 1984). In previous work on electrical impedance in leaves (Greenham *et al.*, 1972, 1978, 1980), electrode impedance was not effectively eliminated. In this study, we use multiple inter–electrode spacings, providing concentric (multi-circular) measurements, to eliminate electrode impedance. We present leaf tissue impedance in the form of specific impedance, which is more meaningful than relative values because the effects of leaf thickness and electrode position are eliminated. We also examine tissue damage due to insertion of electrodes and the effect of impedance measurement due to tissue damage.

MATERIALS AND METHODS

Materials and treatment

Peperomia obtusifolia and *Brassica oleracea* (cabbage) were grown in soil in pots in a greenhouse at Dalhousie University under natural light condition. In the case of *P. obtusifolia*, the leaves were taken from a 30 cm high plant. In the case of *B. oleracea*, leaves were taken from plants grown for 8 weeks.

In compiling Table 1, leaves 1, 2, 4, 7, 10, 14, and 15 from the bottom were selected from four plants. For freeze–thaw

[1] To whom correspondence should be addressed.

stress experiments (Table 2) the 2nd leaves from the bottom were selected from another four plants. Each leaf was halved; one half was left at room temperature for 6 h and the other half was frozen at −3 °C for 3 h and then cooled to −6 °C at a rate of 4·8 °C h^{-1} using a circulating bath (for full description of the freezing facility, see Zhang and Willison, 1990). Thawing was completed at room temperature for 2 h.

The impedance of a laminar tissue

In a relatively uniform plant tissue, specific impedance Z_0 (ohm cm) is approximately the same everywhere. For a laminar tissue with a thickness H (Fig. 1), if one electrode is inserted centrally and another electrode, in the form of a surrounding ring, is spaced some distance (r) from the centre, the total impedance between the 'central electrode' and the 'ring electrode' can be calculated as follows.

The laminar tissue between the central electrode and the ring electrode can be regarded as the sum of many concentric thin cylinders of height H (Fig. 1). For a cylinder with radius r and thickness dr (which is very small), the impedance between the inside surface and outside surface of the cylinder is proportional to dr (along the direction of the electrical field), and inversely proportional to the surface area of one side (outer surface or inner surface) of the cylinder, $2\pi rH$, i.e.

$$dZ_t = \frac{Z_0 dr}{2\pi rH}. \quad (1)$$

As dZ_t is inversely proportional to r, a cylinder closer to the central electrode will have a greater impedance than a cylinder of the same thickness further from the central electrode. The total impedance of this laminar tissue between the central electrode and the ring electrode is the sum of all cylinder impedance dZ_t's in series, or the integration of Eq. (1):

$$Z_t = \frac{Z_0}{2\pi H}\int_{r_1}^{r_2}\frac{dr}{r} = \frac{Z_0}{2\pi H}\ln\left(\frac{r_2}{r_1}\right)$$

or

$$Z_t = A\ln(r_2/r_1). \quad (2)$$

in which $A = Z_0/(2\pi H)$, r_1 is the radius of the central electrode and r_2, the radius of the ring electrode (Fig. 1).

Separation of tissue impedance from electrode impedance

If a two-terminal electrode arrangement is used, the impedance measurement contains electrode impedance (Stout *et al.*, 1987; Zhang and Willison, 1991*a*, *b*). With an electrode impedance Z_e, the total measured impedance is

$$Z = Z_e + A\ln(r_2/r_1). \quad (3)$$

In Eq (3), Z_e and A can be determined from a series of Z values measured at different r_2 values, based on linear least squares (regarding $\ln(r_2/r_1)$ as a variable) (Stout *et al.*, 1987; Zhang and Willison, 1991*a*, *b*). The specific tissue impedance Z_0 is given by

$$Z_0 = 2\pi HA. \quad (4)$$

Impedance measurement and analysis

I. Electrode arrangement: The electrode arrangement was based on that described by Greenham *et al.* (1972). Four stainless steel entomological pins (radius 0·035 cm) were used: one pin as a 'central electrode' and the other three, which were interconnected with copper wire, as a 'ring electrode' (Fig. 2). Several concentric measurements were made in each leaf. In large leaves, the radius r_2 varied from 3 mm to 30–40 mm and up to 5 measurements at different inter–electrode spacings were made. In smaller leaves, the radius varied from 3 mm to 15–20 mm and only 3 inter-electrode spacings could be measured.

II. Impedance measurement: Electrical impedances were measured with a microcomputer controlled HP Precision LCR meter (model 4284A) (Zhang and Willison, 1991*b*). In the experiment to test 'Tissue damage by electrode insertion, Part II: Effect of electrode size on impedance', larger central electrodes were created. Figure 3 shows an electrode configuration in which the radius of the effective central electrode is relatively large (3 mm). In this case, the central electrode consists of three pins that are interconnected (Fig. 3).

III. Impedance analysis: Impedance spectra measured at different r_2's, in a single leaf, were analysed to determine the tissue impedance spectrum and the electrode impedance spectrum. Analysis of the tissue impedance spectrum was made with a program 'MODEL3' (Zhang and Willison, 1992*a*) to determine the various components of a double shell model (Fig. 4) which correspond to extracellular resistance (R_1), cytoplasmic resistance (R_2), vacuole interior resistance (R_4), plasma membrane capacitance (C_3), and tonoplast capacitance (C_5) (Zhang and Willison, 1991*a*).

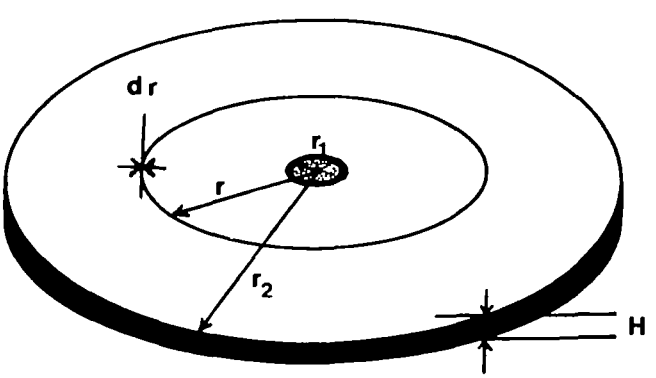

FIG. 1. A disc of laminar tissue with thickness H. r = Radius of an imaginary cylinder around the central electrode; dr = thickness of the imaginary cylinder; $2\pi rH$ = radial surface area of the cylinder.

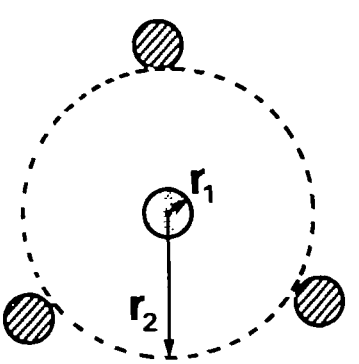

FIG. 2. Electrode configurations. One pin as the central electrode and the other three as the ring electrode; r_1 is the radius of the central electrode and r_2 is the radius of the ring electrode.

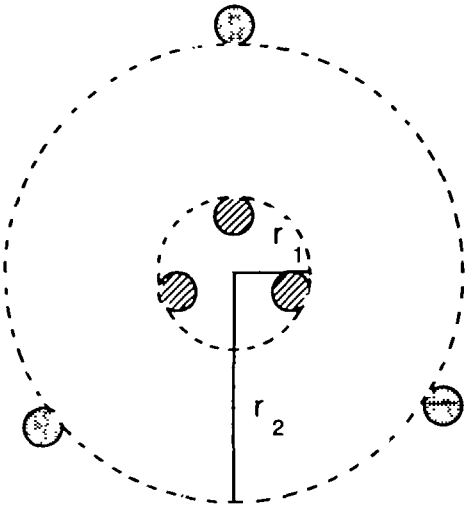

FIG. 3. A disc of leaf in impedance measurement with a relatively large radius of the central electrode (3 mm). Three pins (each with radius of 0·35 mm) were interconnected by copper wire to act as one central electrode.

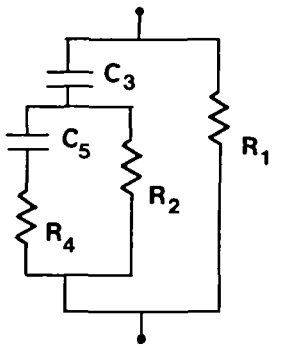

FIG. 4. A double shell model. R_1 = extracellular resistance; R_2 = cytoplasmic resistance; R_4 = vacuole interior resistance; C_3 = plasma membrane capacitance; C_5 = tonoplast capacitance.

Water content

The fresh weights of *B. oleracea* leaves were measured immediately after impedance measurements. The dry weights were measured after leaving the leaves in an 80 °C oven for 24 h.

Tissue damage by electrode insertion

Part I: Calculating the damage effect in the impedance equations (Hypothesis): When an electrode is inserted into plant tissue, a collar of damaged tissue is created around the electrode (Fig. 5). In Fig. 5, r_1 and r_2 are the same as in Eq. (3). In addition, the diagram shows r'_1 which represents a hypothetical range of tissue damage due to insertion of the central electrode, the damaged tissue being that which lies between r_1 and r'_1 (Fig. 5). Although tissue damage due to electrode insertion should be the same when caused by either the central electrode or any pin in the ring electrode, only damage produced by the central electrode is considered here. As seen in Eq. (3), damage around the central electrode has a much greater effect on the calculation than the same amount of damage around pins in the ring electrode, when $r_1 \ll r_2$.

Because damaged tissue has a much lower impedance than normal living tissue (Hayden *et al.*, 1969; Stout, 1988; Zhang and Willison, 1992*a*), the damaged region around the central electrode can be regarded as an extension of the central electrode. Accordingly, r'_1 should replace the r_1 in Eq. (3), i.e.

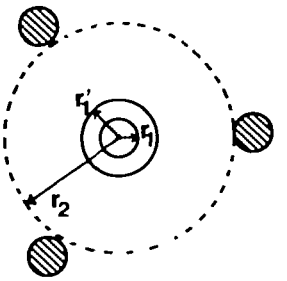

FIG. 5 A disc of leaf in impedance measurement. r_1 is the radius of the central electrode and r_2 is the ring electrode. The area between r_1 and r'_1 represents tissue damage due to insertion of the central electrode.

$$Z = Z_e + A \ln(r_2/r'_1). \quad (5)$$

In Eq. (5), Z_e is the electrode impedance. It includes the contribution made by the damaged tissue (let us call this 'actual electrode impedance'). In reality, r'_1 is unknown and it must be guessed.

In Eq. (3), r_1 was effectively used as a guess for r'_1. When there is tissue damage,

$$r'_1 = br_1 \ (b > 1).$$

From Eq. (5)

$$Z = [Z_e - A \ln(b)] + A \ln(r_2/r_1) \quad (6)$$

in which Z_e is the actual electrode impedence calculated by Eq. (5) and the component $[Z_e - A \ln(b)]$ is the estimated electrode impedance using Eq (3).
Since $b > 1$, $\ln(b) > 0$, then

$$Z_e - A \ln(b) < Z_e. \quad (7)$$

Equation (7) shows that the electrode impedance $[Z_e - A \ln(b)]$ estimated by Eq. (3) is smaller than the actual electrode impedance Z_e. When $A \ln(b) > Z_e$, $[Z_e - A \ln(b)]$ will be negative. However, the tissue impedance related parameter, A, remains the same in both Eq. (3) and Eq. (5). Therefore, the specific tissue impedance Z_0 is not affected by errors in guessing r'_1.

Tissue damage by electrode insertion

Part II: Effect of electrode size on impedance: The following is a corollary of the hypothesis in Part I.

In Eq. (7), a decrease in the coefficient b will reduce the difference between the electrode impedance $[Z_e - A \ln(b)]$ estimated by Eq. (3) and the actual electrode impedance Z_e. If the width of tissue damage caused by insertion of the central electrode (indicated by $r'_1 - r_1$ in Fig. 5) is independent of the radius of that electrode, we should obtain the actual electrode impedance, Z_e, by Eq. (3) at a radius of the central electrode (r_1) at which $b = 1$. In practice, as the radius of the central electrode (r_1) increases, the electrode impedance $[Z_e - A \ln(b)]$ estimated by Eq. (3) should approach the actual electrode impedance Z_e. An experiment to test this corollary will, therefore, further test the original hypothesis in 'Tissue damage by electrode insertion'.

RESULTS

Tissue impedance properties

A directly measured impedance spectrum (at any single r_2 which included the electrode impedance spectrum), in either *P. obtusifolia* leaf or *B. oleracea* leaf, had a characteristic pattern. In a Cole–Cole plot, it was an incomplete semicircle with a straight line pointing to the upper right (Fig. 6A, B). The greater the r_2 the higher were both the resistance and reactance at any particular frequency (Fig. 6A, B). When the spectra measured at several different r_2 values were subjected to analysis with linear least squares, the tissue impedance spectra could be obtained (Fig. 7A, B).

The tissue impedance spectra in *P. obtusifolia* leaf did not vary much from sample to sample throughout the range of 100 Hz–800 kHz and, therefore, the whole spectrum can be subjected to analysis in relation to the double shell model (Fig. 4). In *B. oleracea* leaves, sample-to-sample variations in tissue impedance in the range 100 Hz–1 kHz were found. Because these variations could not be explained, only the data from 1 kHz to 800 kHz were analysed. Similar inter–sample variations were also found in thin leaves of other species such as *Pelargonium* sp. (Geranium) (data not shown).

The double shell model fitted well to impedance spectra measured in leaves of both *P. obtusifolia* (Fig. 7A) and *B. oleracea* (Fig. 7B). The fit was better in *P. obtusifolia* than in *B. oleracea* (cf. Fig. 7A and B).

When impedance data from *B. oleracea* leaves were analysed in relation to the double-shell model, it was found that (i) resistances were lower and capacitances were higher in younger leaves than in older leaves (Table 1); (ii) the correlation between percentage water content and any model parameter was poor (data not shown); (iii) resistances were lower in leaves subjected to a −6 °C stress than in non-stressed leaves (Table 2), even though there was no change in outward appearance of the leaves following −6 °C stress.

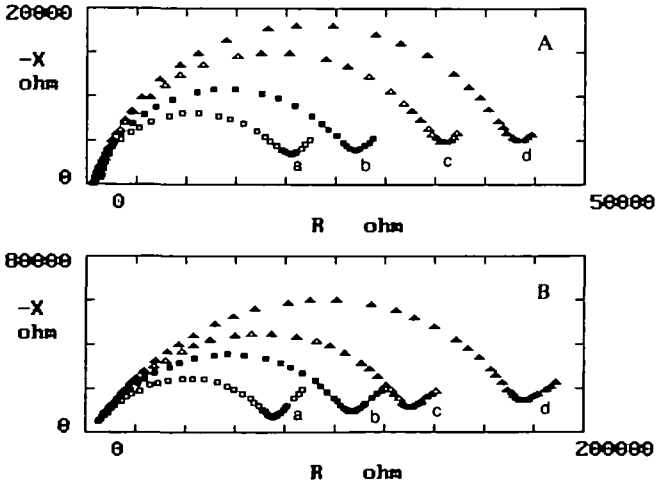

FIG. 6. Examples of impedance spectra, in Cole–Cole plot, measured in a *P. obtusifolia* leaf (A) and a *B. oleracea* leaf (B). (A). r_1 = 0·35 mm, r_2 = 3, 6, 12, and 18 mm for curves 'a', 'b', 'c' and 'd', respectively. Leaf thickness 1·5 mm. (B). r_1 = 0·35 mm, r_2 = 3, 6, 12, and 24 mm for curves 'a', 'b', 'c' and 'd', respectively. Leaf thickness 0·5 mm.

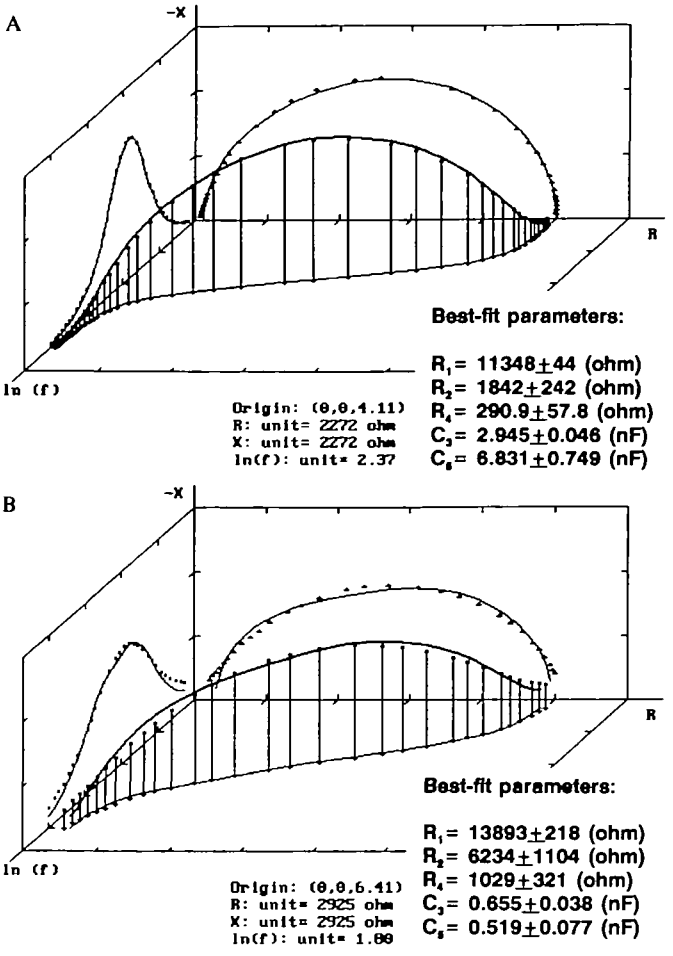

FIG. 7. Tissue impedance spectrum from *P. obtusifolia* leaf (A) and *B. oleracea* leaf (B) and the corresponding curve-fit by double shell model to these spectra. In both (A) and (B), scattered data are from experiments and continuous lines are the best fit by the double shell model. (■) 3-D data in the space of R-X-ln(f); (▽) projection of the 3-D data on R-ln(f) plane; (|) projection of the 3-D data on X-ln(f) plane; (△) projection of the 3-D data on R-X plane (the Cole–Cole plot). The number following each parameter is the 95% confidence interval for that parameter.

Electrode impedance properties, Part I

It was consistently found that resistance values were negative and reactance values were positive at many frequencies when the exact radius of the metal central electrode was used in Eq. (3) (Fig. 8).

In a computer simulation, electrode impedance spectra were calculated by Eq. (5) with guessed values of r'_1 (Fig. 9). The objective was to find an r'_1 which produced a hypothetical electrode impedance spectrum that was similar to a typical electrode impedance spectrum found in previous measurements on appropriate materials such

TABLE 1. B. oleracea *leaf development and per cent water content in relation to the double shell model parameters*

All resistances are in ohm cm and all capacitances are in nF cm^{-1}. Standard errors are indicated in brackets. For both per cent water content and double shell model parameters, the averaged data and standard error are calculated from four samples.

Leaf ID	Per cent water content	R_1	R_2	R_4	C_3	C_5
1	78·6	6974	5773	903	0·957	0·574
	(2·3)	(547)	(554)	(31)	(0·19)	(0·062)
2	74·7	5842	5184	832	1·12	0·652
	(1·2)	(326)	(147)	(19)	(0·076)	(0·015)
4	74·6	4688	4111	554	1·77	1·06
	(0·93)	(503)	(518)	(60)	(0·30)	(0·16)
7	76·5	3421	2832	376	2·38	1·47
	(0·59)	(215)	(248)	(28)	(0·33)	(0·16)
10	79·4	3976	3976	428	1·93	1·27
	(0·75)	(403)	(674)	(26)	(0·20)	(0·11)
14	84·0	3632	2255	371	1·81	1·39
	(1·2)	(436)	(374)	(36)	(0·38)	(0·25)
15	84·3	3569	2711	372	1·90	1·36
	(1·1)	(389)	(467)	(27)	(0·36)	(0·16)

TABLE 2. *Double shell model parameter changes in relation to freeze–thaw stress in* B. oleracea *leaves*

All resistances are in ohm cm and all capacitances are in nF cm^{-1}. Standard errors are shown in brackets. The averaged data and standard error are calculated from four samples.

Treatment	R_1	R_2	R_4	C_3	C_5
Control	6413	9141	656	1·16	0·622
	(264)	(1192)	(50·4)	(0·19)	(0·033)
−6 °C	911	1822	313	1·21	0·624
	(124)	(737)	(0·7)	(0·40)	(0·000)

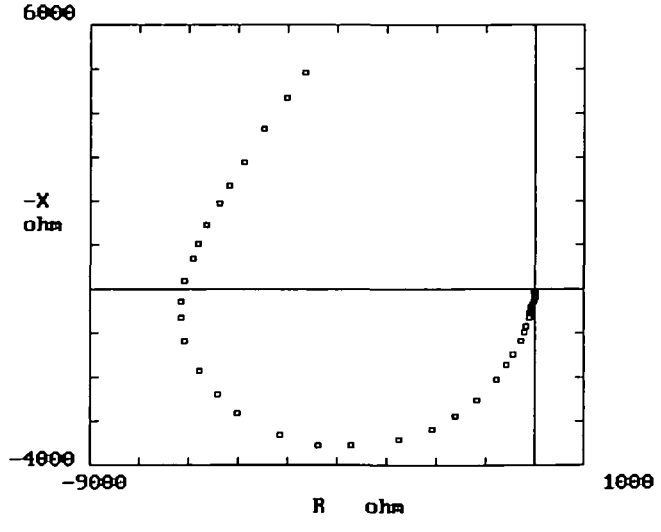

FIG. 8. An electrode impedance spectrum in *P. obtusifolia* calculated by Eq. (3). $r_1 = 0{\cdot}35$ mm. Many resistances are negative and many reactances are positive.

as potato tubers (Zhang and Willison, 1992*b*). The simulation (Fig. 9) shows that when r'_1 is 0·8 mm or more, the simulated spectrum (Fig. 9, curves 'c'–'f') has a similar pattern to that of a typical electrode impedance spectrum

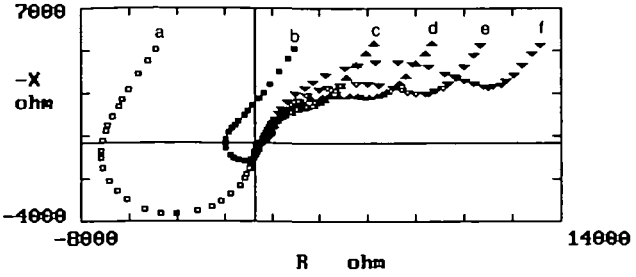

FIG. 9. A simulation with guessed tissue damage (r'_1) resulting from electrode insertion into *P. obtusifolia* leaf. The actual radius of the central electrode is $r_1 = 0{\cdot}35$ mm. Curves 'a', 'b', 'c', 'd', 'e', and 'f' are obtained with r'_1 equal to 0·35 mm, 0·6 mm, 0·8 mm, 1·0 mm, 1·2 mm, and 1·5 mm, respectively. At $r'_1 = 0{\cdot}8$ mm and greater, simulation produces electrode impedance spectra with consistently positive resistance and negative reactance.

in electrolytic solution (Bard and Faulkner, 1980) or in potato tuber (Zhang and Willison, 1992*b*). The width of the surrounding collar which contributes to electrode polarization is, therefore, probably at least 0·4–0·5 mm in *P. obtusifolia* leaves (in the case of Fig. 9, curve 'c', $r'_1 = 0{\cdot}8$ mm and $r_1 = 0{\cdot}35$, the damaged zone is $r'_1 - r_1 = 0{\cdot}45$ mm wide). It was later found that insertion of an electrode in some *P. obtusifolia* leaves produced visible damage (Fig. 10). The damaged zone surrounding the 0·35 mm electrode shown in Fig. 10 is about 0·4 mm wide.

Electrode impedance properties, Part II

A typical example of an electrode impedance spectrum in *B. oleracea*, using measurement with the large-radius electrode configuration in Fig. 3 and calculation by Eq. (3), is shown in Fig. 11. As expected, the spectrum is similar to a typical acceptable electrode impedance spectrum (Bard and Faulkner, 1980; Zhang and Willison, 1992*b*).

In 'Part I' of the 'tissue damage by electrode insertion', the hypothesis is supported by the simulation which shows that the effective radius of the central electrode is underestimated (Fig. 9). If this hypothesis is correct, we should also be able to transform an acceptable electrode impedance spectrum into an erroneous spectrum, such as that in Fig. 8, by setting the radius of the central electrode to a less-than-true value during calculation using Eq. (3). Figures 11 and 12 show the contrast between an acceptable electrode impedance spectrum obtained from a specimen (Fig. 11) and the transformed spectra which are obtained when recalculated using various r_1 values in Eq. (3) (Fig. 12).

The simulation (Fig. 12) shows that if r_1 values are smaller than the true radius of the central electrode (3·0 mm), the erroneous electrode impedance spectra which arise are similar to those obtained when the pin radius (0·35 mm) was used in Eq. (3) (e.g. Fig. 8). This confirms the prediction that an acceptable electrode impedance spectrum can be transformed into an errone-

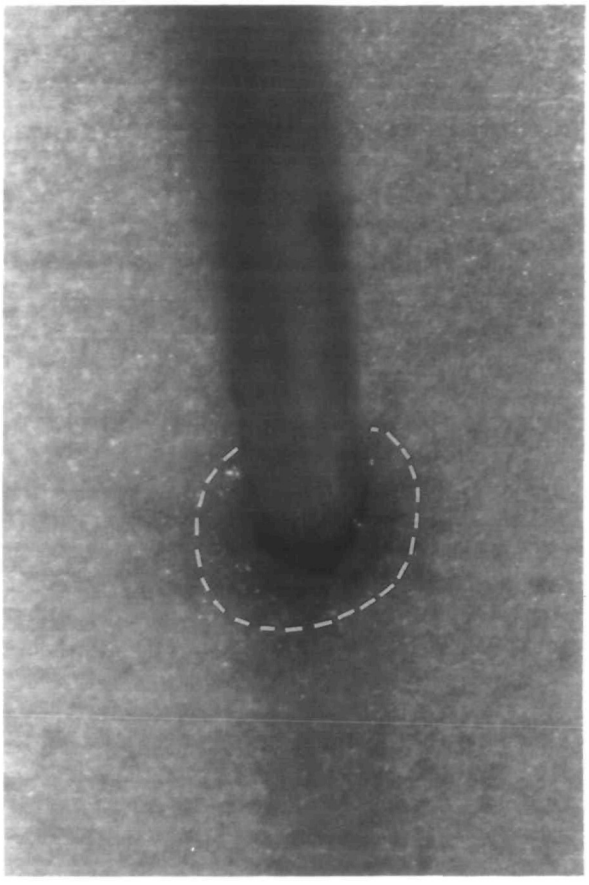

FIG. 10. A photograph showing visible damage caused by electrode insertion into *P. obtusifolia* leaf. The radius of the electrode is 0·35 mm and the width of the zone of damage around the electrode is about 0·4 mm, as indicated by the dotted line.

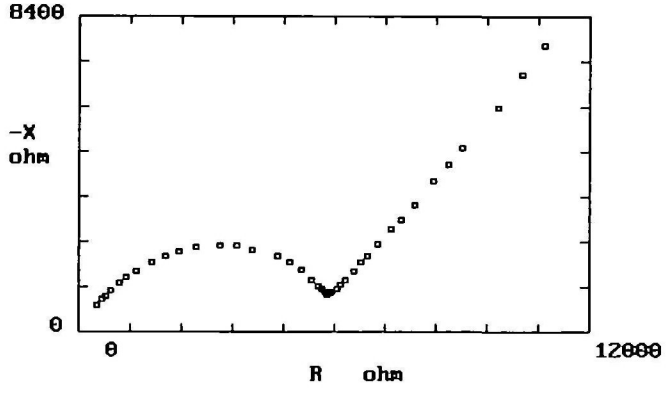

FIG. 11. An electrode impedance spectrum in *B. oleracea* leaf measured with the electrode configuration in Fig. 3. and calculated by Eq. (3). $r_1 = 3{\cdot}0$ mm.

ous spectrum just by setting the radius of the central electrode to a less-than-true value. This is further support for the hypothesis in 'Part I'.

Figure 12 also shows that when a larger r_1 value (3·5 mm, 4·0 mm or larger) was used, the electrode impedance spectrum calculated was similar in pattern to that

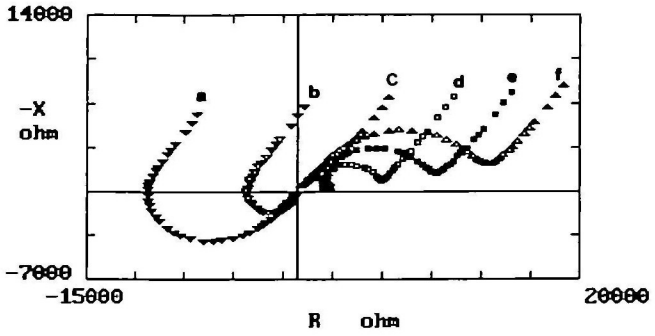

FIG. 12. Simulated electrode impedance spectra with various r_1' values in *B. oleracea* leaf. The actual radius of the central electrode is $r_1 = 3{\cdot}0$ mm. Curves 'a', 'b', 'c', 'd', 'e', and 'f' are obtained with r_1 equal to 1·5 mm, 2·0 mm, 2·5 mm, 3·0 mm, 3·5 mm, and 4·0 mm, respectively. *When r_1' is smaller than the real radius of central electrode (3·0 mm),* simulation produces erroneous electrode impedance spectra (curves 'a'–'c') that appear similar to those measured with a 0·35 mm radius central electrode (see Fig. 8). At r_1' larger than the real radius of the central electrode, simulation produces similar electrode impedance spectral pattern (curves 'e'–'f') as that produced with the correct radius of the central electrode (3·0 mm).

with $r_1 = 3{\cdot}0$ mm. This would suggest that it is possible to estimate a lower limit for the width of the collar of damaged tissue, but that an upper limit cannot be estimated. In the cases measured in this work, this collar was at least 0·4–0·5 mm wide.

DISCUSSION

The potential usefulness of the measurement of impedance in leaves and its analysis was demonstrated by Greenham and co-workers in works concerned with taxonomy (Greenham *et al.*, 1972, 1980) and virus infections (Greenham *et al.*, 1978). In the present work, the basic technique has been improved by (i) using a broader frequency range (100 Hz to 800 kHz) than the 10 kHz to 200 kHz used by Greenham and co-workers; (ii) using more frequency points (40) than the four used by Greenham and co-workers; (iii) measuring impedance at 3–5 inter-electrode spacings (r_2) and using this to eliminate electrode impedance. While the works of Greenham and colleagues (1972, 1978, 1980) probably indicate real differences among the specimens tested, their use of a fixed spacing between two electrodes made it impossible for them to eliminate electrode impedance. Given the inclusion of this unknown non-physiological variable in their data, their conclusions must be considered tentative.

Tissue impedance properties

The impedance spectra obtained from leaves are similar to those from other plant materials previously studied (Zhang and Willison, 1991*a*, *b*, 1992*a*, *b*), the Cole–Cole plot being almost a semicircle (Fig. 7A, B). A difference which may be important is that in *B. oleracea* leaves, as well as similar thin leaves from other species such as *Pelargonium* sp. (Geranium), there was unexplainable

inter-sample variation in the low frequency range (100 Hz–1 kHz). Further experimentation may permit the source of this variation to be identified and to be interpreted usefully, if it is not artifactual.

As with organs like potato tuber and carrot root (Zhang and Willison, 1991*a*), the results described in the present paper indicate that plant leaf tissue can be represented by the double shell model (Fig. 7A, B). Our measurements of impedance in relation to developmental stage and freezing injury in *B. oleracea* were planned as simple and preliminary indications of the utility of this technique in physiological studies. The data in Table 1 indicate that resistances tended to be higher but capacitances tended to be lower at later developmental stages of leaves (assuming that leaf age rather than time of initiation is most significant). While these data have little physiological significance in the absence of correlative data other than percentage water content, they do show that the technique has the capacity to provide significant differences within a data-set of model parameters obtained from a developmental series. The observation that resistances dropped significantly following −6 °C freeze–thaw stress in *B. oleracea* leaves (Table 2), despite the absence of damage by visual estimation, also indicates the utility of the technique in plant stress physiology. This finding accords well with the findings of Zhang and Willison (1992*a*) on impedance changes in carrot root tissue subjected to non-lethal freeze–thaw stress. The results indicate the presence of sublethal injury which is not readily detectable by other means (for discussion, see Zhang and Willison, 1992*a*).

Electrode impedance properties

There is enough evidence to support the hypothesis that electrode insertion produces a 0·4–0·5 mm collar of damage in leaf tissue around a 0·35 mm radius electrode. The current hypothesis explains the unreasonable electrode impedance spectra obtained by using Eq. (3) (Fig. 8). On the other hand, the impedance technique is capable of detecting the approximate degree of tissue damage which is usually non-detectable by other techniques. In earlier works by Greenham and co-workers (1972, 1978, 1980), neither electrode impedance properties nor tissue damage around electrodes was studied. In their work, Greenham and colleagues (1972, 1978, 1980) used a 2 mm inter-electrode spacing. According to the present results, a significant proportion (50%) of their tissue under measurement may have been damaged by electrode insertion.

ACKNOWLEDGEMENT

This research was supported by NSERC (Canada).

LITERATURE CITED

ACKMANN JJ, SEITZ MA. 1984. Methods of complex impedance measurements in biological tissue. *CRC Critical Reviews in Biomedical Engineering* **11,** 281–311.

BARD AJ, FAULKNER LR. 1980. *Electrochemical methods—fundamentals and application*. John Wiley & Sons, Inc., 316–67.

FERRIS CD. 1974. *Introduction to bioelectrodes*. New York and London: Plenum Press, 9–41.

GREENHAM CG, GROVES RH, MULLER WJ. 1980. Variation between populations of one form of skeleton weed (*Chondrilla juncea* L.) shown by electrical parameters. *Journal of Experimental Botany* **31,** 967–74.

GREENHAM CG, HELMS K, MULLER WJ. 1978. Influence of virus infections on impedance parameters. *Journal of Experimental Botany* **29,** 867–77.

GREENHAM CG, HULL VJ, WARD MM. 1972. Electrical characteristics as discriminant criteria for three forms of skeleton weed (*Chondrilla juncea* L.). *Journal of Experimental Botany* **23,** 210–15.

HAYDEN RI, MOYSE CA, CALDER FW, CRAWFORD DP, FENSOM DS. 1969. Electrical impedance studies on potato and alfalfa tissue. *Journal of Experimental Botany* **20,** 177–200.

REPO T, TUOVINEN T, SAVOLAINEN T. 1990. Estimation of an electrical model of plant tissue using the impedance locus. *Silva Carelica* **15,** 51–9.

SCHWAN HP. 1963. Determination of biological impedances. In Nastuk WL, ed. *Physical techniques of biological research*, Vol. 6. New York: Academic Press, 323–407.

STOUT DG. 1988. Effect of cold acclimation on bulk tissue electrical impedance. I. Measurements with birdsfoot trefoil at subfreezing temperatures. *Plant Physiology* **86,** 275–82.

STOUT DG, HALL JW, MCLAUGHLIN NB. 1987. *In vivo* plant impedance measurements and characterization of membrane electrical properties: the influence of cold acclimation. *Cryobiology* **24,** 148–62.

WILNER J, BRACH EJ. 1979. *Utilization of bioelectric tests in biological research*. Engineering and Statistical Research Institute, Canada.

ZHANG MIN, WILLISON JHM. 1990. Electrical conductance of red onion scale tissue during freeze–thaw injury. *Acta Botanica Neerlandica* **39,** 359–67.

ZHANG MIN, WILLISON JHM. 1991*a*. Electrical impedance analysis in plant tissues: A double shell model. *Journal of Experimental Botany* **42,** 1465–76.

ZHANG MIN, WILLISON JHM. 1991*b*. A microcomputer-based precision impedance analyser for measuring electrical impedance in plant tissues. *Canadian Journal of Plant Science* **71,** 1285–8.

ZHANG MIN, WILLISON JHM. 1992*a*. Electrical impedance analysis in plant tissues: The effect of freeze–thaw injury on the electrical properties of potato tuber and carrot root tissues. *Canadian Journal of Plant Science* **72,** 545–53.

ZHANG MIN, WILLISON JHM. 1992*b*. Electrical impedance analysis in plant tissues: *in vivo* detection of freezing injury. *Canadian Journal of Botany* **70,** 2254–8.